FINITE ELEMENT ANALYSIS OF CONFINED CONCRETE COLUMNS

Christina Claeson
Ph.D.
Division of Concrete Structures
Chalmers University of Technology
S-412 96 Göteborg, Sweden

ABSTRACT

Finite element analyses of confined columns are presented. Based on a confinement dependent uniaxial concrete model, the importance of the yield strengths of the stirrups and the longitudinal reinforcement bars, the spacing of the stirrups, and the configuration of the cross-section, in combination with different load eccentricities are evaluated. It was found that the spacing of the stirrups and the reinforcement configuration are of the greatest importance for the post-peak behavior. To achieve ductile structural behavior of high-strength concrete columns, a higher value of the volumetric stirrup ratio is required.

Key words: Confined columns, Finite element analysis, High-strength concrete

1. INTRODUCTION

There are many advantages in using a high-strength concrete instead of a normal-strength concrete, especially the increase in compressive strength and the higher durability. However, due to the brittleness of high-strength concrete, many engineers are still reluctant to use it in structures. If this problem with brittleness could be reduced or even overcome, many advantages would be gained. Confinement has a significant influence on ductility in columns. Well-confined columns imply high ductility, whereas lightly confined columns imply the opposite. Much effort has gone into studying the effect of confinement in both high-strength concrete and normal-strength concrete columns. As a result of these studies, material models that take into account the effect of confinement have been proposed: for example Park, Priestley and Gill /1/; Sheikh and Uzumeri /2/; Yong, Nour and Nawy /3/; Bjerkeli, Tomaszewicz and Jensen /4/; Madas and Elnashai /5/; and Cusson and Paultre /6/. While a 3-D material model can present detailed information about the stress-state in all members, in many cases a confinement-dependent uniaxial constitutive model is sufficiently accurate. Using a model of this type, it is possible to identify the parameters of importance in the design of ductile columns.

This paper describes the numerical analyses of confined columns using the non-linear finite element program ABAQUS /7/ with a confinement material model included. This model takes into account the different stress-strain curves of the concrete cover and the confined core. A parametric study was carried out, the aim of which was to determine whether high-strength

concrete columns can obtain a less brittle failure by appropriate reinforcement configuration. It evaluates the importance of the yield strengths of the stirrups and the longitudinal reinforcement bars, the spacing of the stirrups, and the configuration of the cross-section, in combination with different load eccentricities.

2. TEST PROGRAM

From a test series carried out at the Division of Concrete Structures, Chalmers University of Technology, three short stub columns and two slender columns were selected for the verification of the finite element (FE) model. The details of these specimens are shown in Figure 1 and Table 1. The compressive cylinder strength, f_{co}, refers to compression tests on specimens of sizes $\phi 150 \times 300$ mm, e is the eccentricity of the applied axial load, f_{sy} the yield strength of the longitudinal bars and s is the stirrup spacing. The clear concrete cover to the stirrups was 15 mm for columns no. 1, 2, 4 and 5, and 10 mm for column no. 3. Further data about the test specimens are found in Claeson /8/.

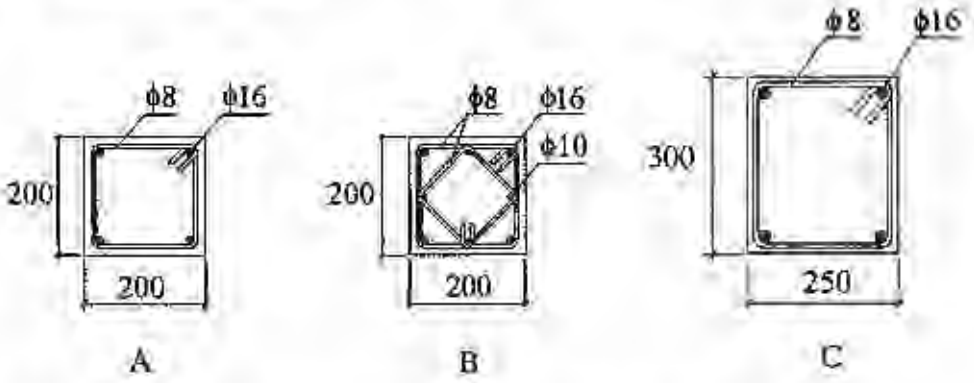

Figure 1 Concrete columns: geometry and details of configurations A, B and C.

Table 1 Details of selected specimens

Column	Dimensions [mm]	f_{co} [MPa]	e [mm]	f_{sy} [MPa]	s [mm]	Reinforcement configuration	Max. load [kN]
1	200 × 200 × 800	91	0	636	130	A	3920
2	200 × 200 × 800	33	0	636	130	A	1650
3	250 × 300 × 900	112	90	636	50	C	3064
4	200 × 200 × 3000	91	20	636	130	A	2310
5	200 × 200 × 3000	33	20	636	130	A	990

3. MATERIAL MODEL

3.1 General

The structural behavior of a column depends on the load eccentricity. While the load eccentricity is small, the compressive behavior of the concrete is dominant. Therefore, it is important to accurately model the phenomena associated with compression, such as gradual spalling of the concrete cover and the confining action of the stirrups. As the load eccentricity increases, tensile cracking gradually dominates and the properties of the reinforcing steel become important. Comparisons of different compressive concrete models applied to test results have shown that the material model proposed by Cusson and Paultre /6/ for high-strength concrete captures the desired features well (Mustapha /9/, Cusson and Paultre /6/, and Oresten /10/). Accordingly, this model has been used for concrete in compression in the following analyses. In the failure of reinforced members, the reinforcement cage, separating the concrete core and cover, can form a natural plane of separation. This seems to be the weakest part of many specimens, especially for high-strength concrete columns. A limitation of the material model is that it does not take account of the premature buckling of the concrete cover in pure compression. However, when the eccentricity of the load increases, the tendency of the cover to buckle decreases. In tension, the tensile softening relation is described using the fracture energy of the concrete.

3.2 Concrete in compression

The material model for concrete used in this analysis is based on a model suggested by Cusson and Paultre /6/. In this model, the determination of the strength and ductility of confined concrete is based on the calculation of the effective confinement pressure using static equilibrium and the concept of the effectively confined concrete area. This model takes into account the different stress-strain curves of the concrete cover and the confined core. Furthermore, it does not assume that the stirrup yields; it estimates the actual stress in the stirrups at peak concrete stress. These features made it attractive to use in the analysis for concrete in compression. An example of stress-strain curves for unconfined and confined concrete is shown in Figure 2.

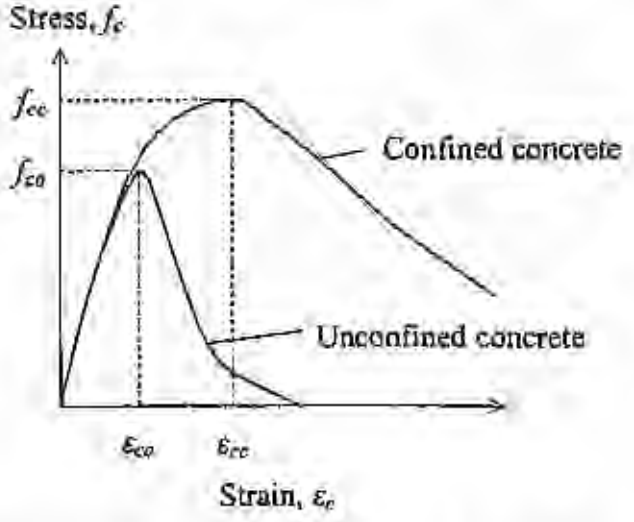

Figure 2 Stress-strain curves for confined and unconfined concrete

The combination of lateral pressure from the confining reinforcement cage and the uniaxial compression generates a triaxial stress state that counteracts the lateral expansion of concrete. Richart et al. /13/ found that the lateral pressure f_l greatly enhanced the maximum strength of a confined concrete. They proposed the relation $f_{cc} = f_{co} + 4.1\ f_{le}$, where f_{co} is the unconfined concrete strength. This relation formed the basis for requirements for confining steel in the ACI Code /14/. Over the years, this relation has been modified although the basic philosophy still remains the same. The increase in strength f_{le} due to the confining steel may be computed as

$$f_{le} = K_e f_l \tag{1}$$

where K_e depends on the geometry of the cross-section and the reinforcement configuration, and f_l is a function, based on equilibrium, of the stress in the transversal bars and the reinforcement configuration. The equation for K_e is

$$K_e = \frac{\left(1 - \frac{\sum \omega_i^2}{6(c_x + c_y)}\right)\left(1 - \frac{s'}{2c_x}\right)\left(1 - \frac{s'}{2c_y}\right)}{(1 - \rho_g)} \tag{2}$$

where ω_i is the clear horizontal spacing between longitudinal bars, c_x and c_y are the dimensions of the concrete core, s' is the clear vertical spacing between the stirrups, and ρ_g is the volumetric ratio of the longitudinal steel with respect to the volume of the concrete core. The confinement effectiveness coefficient, K_e, is of importance when determining the effects of different reinforcement configurations and stirrup spacings. The lateral confining stress on the concrete (total transverse bar force divided by the vertical area of confined concrete) is given as

$$f_l = \rho_{stirrup} f_{hcc} \tag{3}$$

where $\rho_{stirrup}$ is the volume of stirrups and f_{hcc} the actual stress in the stirrups. For further information about the model, the reader is referred to Cusson and Paultre /6/ and Légéron and Paultre /15/.

3.3 Concrete in tension

The smeared crack approach has been chosen to model cracked reinforced concrete, see Hillerborg, Modéer and Petersson /16/. Prior to cracking, concrete can be modeled sufficiently accurately as a linear elastic material. Once cracking has occurred, the stress decreases gradually to zero with increasing crack width. The area underneath the σ-w curve equals the fracture energy G_f, see Figure 3. The descending branch of the tensile stress-crack opening displacement curve can be formulated in different ways; in the present work the descending branch is formed by two straight lines, see Gylltoft /17/. For reinforced concrete, the tensile strain can be calculated based on an estimated crack spacing. It was found that the value of the ultimate strain had little effect on the load-displacement curves. This is because the failures were dominated by the compression mode. Therefore, the ultimate strain was taken as 0.001 for all concrete strengths. This is a rather rough estimation, which needs to be refined in the future. However, the slope of the high-strength concrete is steeper than that of the normal-strength concrete.

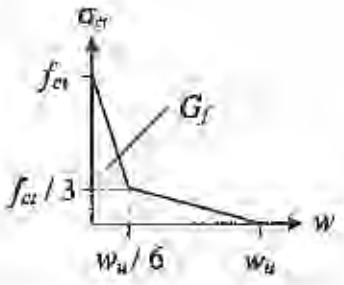

Figure 3 Stress-crack opening relation for the fracture zone.

3.4 Reinforced concrete

To model reinforced concrete, the non-linear finite element program ABAQUS combines standard elements of plain concrete with a special option, called rebar /7/. This option strengthens the concrete in the direction chosen, thereby simulating the behavior of a reinforcement bar. By this approach, the material behavior of the plain concrete can be taken into account independently of the reinforcement.

The behavior of the longitudinal reinforcement bars was simulated using a linear elastic-plastic material model. The modulus of elasticity, the yield strength and the ultimate strength of the reinforcement bars were based on results from tension tests on steel samples from the same batch as the reinforcement bars in the specimens; and the elastic Poisson ratio was approximated to be 0.3. The average properties for ϕ16, ϕ10, and ϕ8 were as follows: (1) yield strength – 636 MPa, 658 MPa and 466 MPa; (2) ultimate strength – 721 MPa, 744 MPa and 607 MPa; and (3) modulus of elasticity – 207 GPa, 213 GPa and 221 GPa.

4. IMPLEMENTATION IN ABAQUS

A material model was coded as a user material subroutine and added to the general-purpose nonlinear finite element package ABAQUS /7/. The proposed material model was designed to be used for beam elements available in the ABAQUS element library. Generally, the beam elements can not include stirrups, which is a disadvantage when modeling concrete columns. However, by including the effect of confinement in the stress-strain curve and giving the confined core and the unconfined cover separate stress-strain curves, a confined concrete column can be analyzed effectively. Two different stress-strain curves for the beam cross section were obtained by identifying each integration point, combining the integration points of the concrete core into one group and the points of the cover into another group, and then assigning each group a material model, see Figure 4. By this approach, the model takes into account the following effects: the complete stress-strain relation of the steel (rebar option), including hardening; the non-linear stress-strain relation for the concrete, including confinement effects in compression and cracking in tension; and changes in the geometry of a section due to progressive spalling of the concrete cover under high strain. However the model does not take into account either the possible buckling of the reinforcement bars or the premature buckling of the high-strength concrete cover.

In the parametric study, three-dimensional two-node hybrid beam elements, B33H, were used. Normally, the model consisted of ten elements along the length of the column.

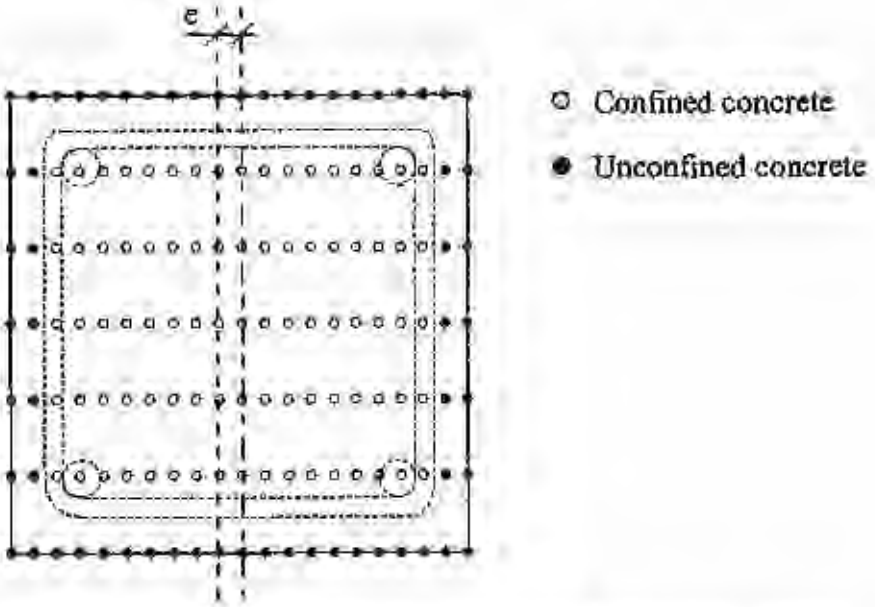

Figure 4 Confined and unconfined integration points in a beam cross-section

5. NUMERIC STUDY

5.1 Verification

Before a parametric study could be carried out, it was necessary to prove that the established finite element model was capable of simulating the structural behavior of short concrete columns. Accordingly, a comparison of load-deflection and load-strain curves from tests and analyses, to validate the accuracy of the model, was carried out. Figures 5, 6 and 7 give the results of the comparison. The results show that the finite element beam model does capture the structural behavior of the columns satisfactorily. However, it was observed that the results from the FE analysis gave a stiffer initial behavior than that of the tests. This discrepancy is attributed primarily to the differences between the measured and modeled geometric and material imperfections. Furthermore, it was observed that the FE analysis gave a higher maximum capacity for the uniaxially compressed concrete columns. It is worth noting that the compressive cylinder values that were used in the analysis of columns no. 1 and 2 may not represent the true values of the concrete columns, due to the size effect and different curing. Richart and Brown stated that the pure compressive value should be multiplied by a coefficient taken as 0.8 to 0.85 /18/. The same range of values for the coefficient was suggested by Hognestad /19/. However, Hognestad also mentioned that this coefficient may vary with concrete strength. Karr, Hanson and Capell /20/ tested higher strength concretes and found that the coefficient should be close to 1.0 for their tests. Mak, Attard, Ho and Darwall /21/ found that the lower boundary ratio of *in situ* effective strength to cylinder strength for the high-strength concretes investigated was generally below 0.85, depending on the size of the cross-section. Clearly, there is still need for more research in this area. For column no. 3 an unreinforced concrete column was cast. The ratio between the column maximum strength and the cylinder strength was found to be 0.9. Accordingly, this value was used in the analysis of column no. 3. In one of the analyses of a normal-strength concrete column, the compressive cylinder strength was reduced 15%. The results of this analysis are included in Figure 6. As can be seen in the figures, $0.85f_{co}$ seems to represent more closely the true concrete strength in the column. However, in the following parametric study the compressive cylinder strength was used for all of the concrete strengths.

In Figures 5a and 6a, the load versus axial displacement relations are shown for both the high-strength and the normal-strength concrete specimens. The results of the tests and the analysis deviate, especially for the normal-strength concrete column. However, when the load versus axial strain relations were plotted in Figures 5b and 6b, the test curves and the results from the analysis coincided approximately on the ascending branch. The measured vertical displacement includes the boundary effect, which explains the deviation of the test and the analysis curves.

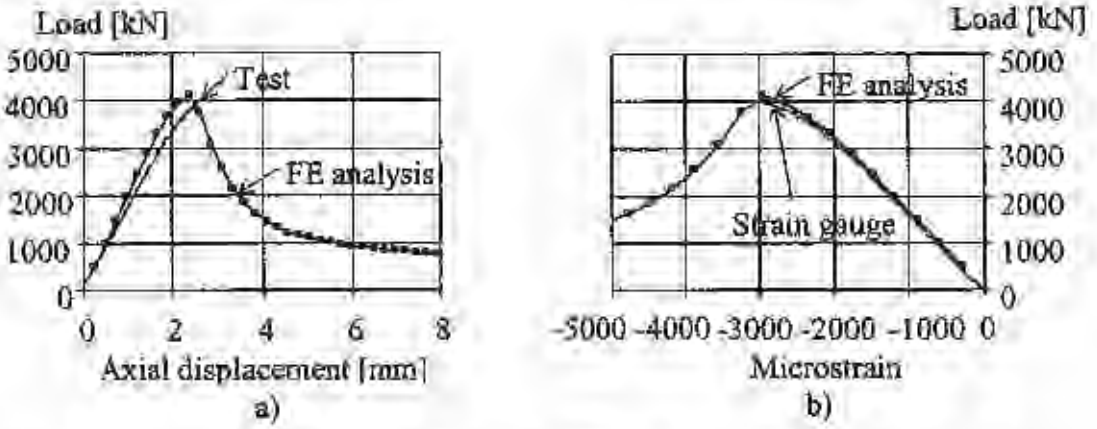

Figure 5 Column no. 1, test results and results of FE analyses: a) Load versus axial displacement curves, and b) Load-vertical strain relations.

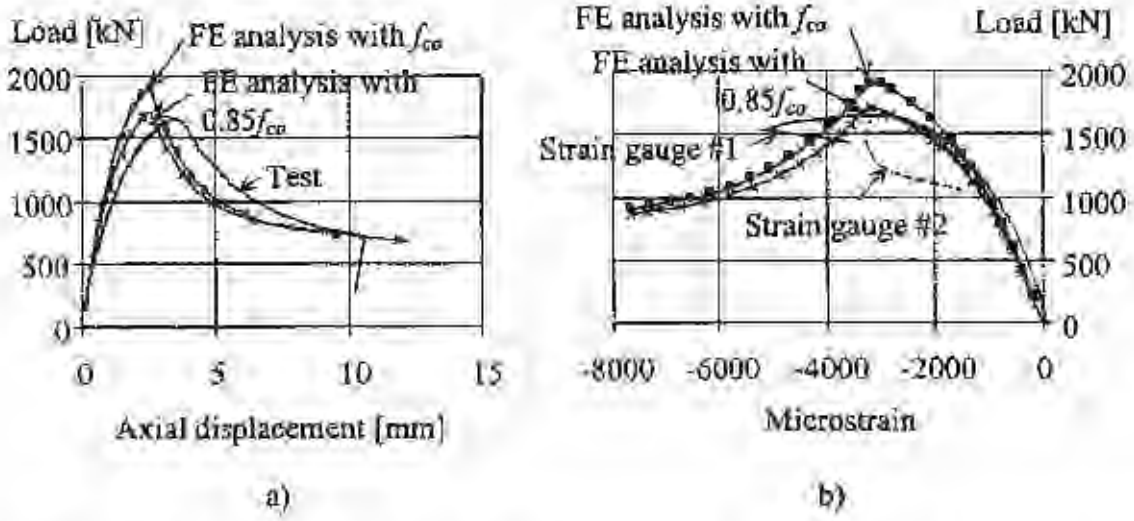

Figure 6 Column no. 2, test results and results of FE analyses: a) Load versus axial displacement curves, and b) Load-vertical strain relations. The figure includes two curves from the FE analysis, one using the cylinder strength and the other $0.85f_{co}$.

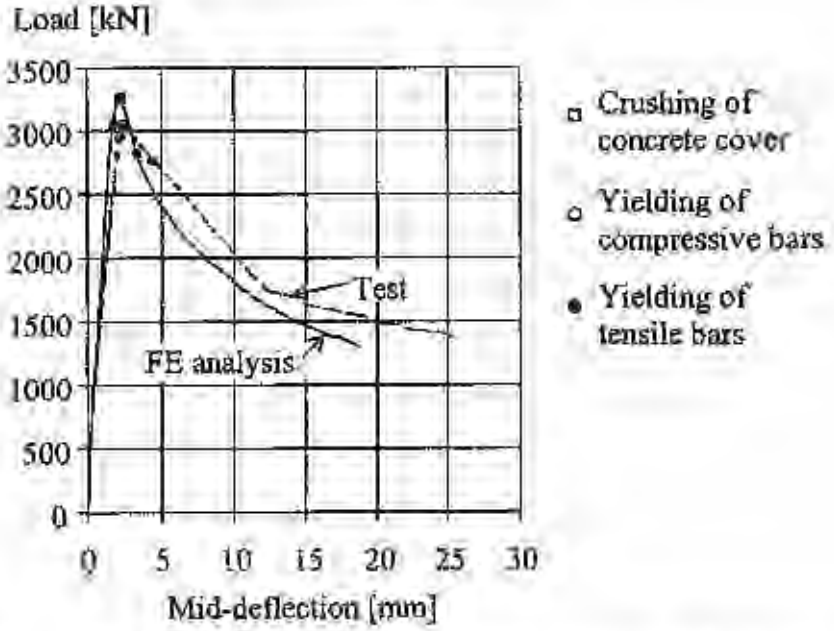

Figure 7 Load versus mid-deflection for high-strength concrete column no. 3 subjected to a load eccentricity of 90 mm.

5.2 Parametric study

The aim of the parametric study was to determine whether a less brittle failure of high-strength concrete columns could be obtained by using a suitable reinforcement configuration. It was also thought desirable to identify what parameter or parameters play a governing role for the post-peak behavior. The six parameters varied in the parametric study are: vertical bar yield strength, stirrup yield strength, stirrup spacing, eccentricity, reinforcement configuration, and concrete compressive strength, see Table 2. The cross-section dimensions were 200 × 200 × 800 mm with reinforcement configuration A or B, see Figure 1. Here, the confinement effectiveness coefficient, K_e, (see equation 2) and the lateral confining stress, f_l, (equation 3) play dominant roles when determining the enhancement of strength for the different reinforcement configurations.

Table 2 Variables in the parametric study

No.	Variable	Value
1	Vertical bar yield strength [MPa]	400, 636
2	Stirrup yield strength [MPa]	400, 500, 600, 1000
3	Stirrup spacing [mm]	50, 100, 150
4	Eccentricity (with and without confinement) [mm]	0, 50, 90
5	Reinforcement configuration	A / B
6	Concrete compressive strength [MPa]	33 / 91

First, a preliminary study was carried out to determine the most important parameters. The results of the preliminary study showed that, although the yield strength of the longitudinal reinforcement bars did have an effect on the maximum load, the effect on the post-peak behavior was insignificant, see Figure 8. Since the yield strength of the reinforcement bars in most of the test specimens was 636 MPa, the yield strength was set to this value in the following studies. Thereafter, all of the variables except the first were combined and analyzed. A column is identified, for example khe50s100400b, in the following manner: k denotes a short column; h denotes high-strength concrete and n normal-strength concrete; e is the eccentricity, in this case 50 mm; s is stirrup spacing, here 100 mm; 400 is the yield strength of the stirrups; and b denotes reinforcement configuration B. The results of the analysis are shown in Figures 9 through 14. Figure 9 shows the load displacement relations for cross-sections with reinforcement configuration A subjected to pure compression. The stirrup spacing was 50 mm and the yield strength of the stirrups ranged from 400 to 1000 MPa for the two concrete strengths. Figure 10 presents the load displacement relations for cross-sections with configuration B subjected to pure compression. For these analyses the stirrup spacing was kept constant at 50 mm and the yield strength varied. Figure 11 shows the load displacement relations for the same cross-sections but with different stirrup spacings and a constant yield strength. In Figures 12 and 13, the cross-sections were subjected to an eccentric compressive axial load. Figure 12 shows the load versus mid-deflection curves for cross-sections of configuration A subjected to a load eccentricity of 50 mm. In the analyses the yield strength of the stirrups was 400 MPa and the stirrup spacing ranged from 50 to 150 mm. In Figure 13, the load deflection relations are shown for cross-sections with configuration A subjected to a load eccentricity of 90 mm. The yield strength was 400 MPa and the stirrup spacing 50, 100 or 150 mm.

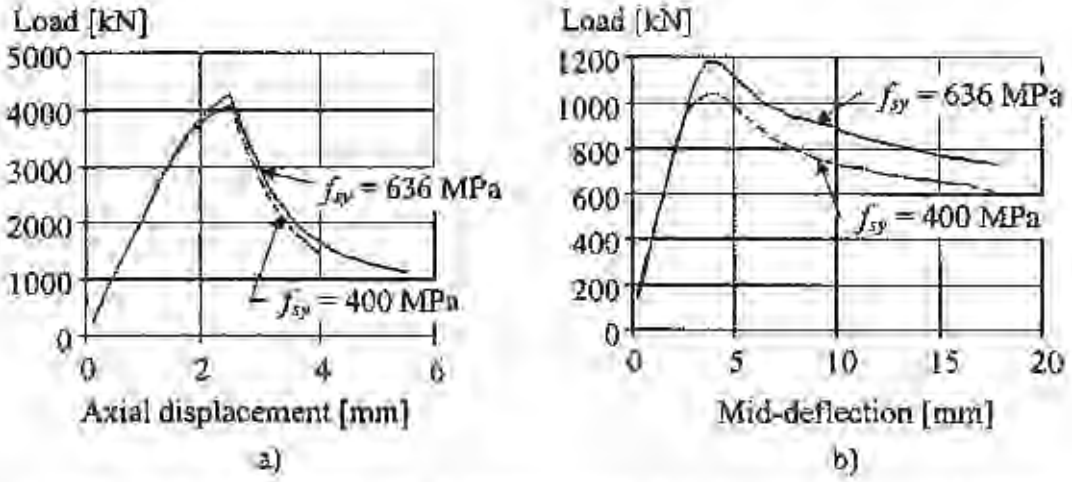

Figure 8 Load-displacement relations for cross-sections with reinforcement configuration A subjected to: a) pure compression, and b) a load eccentricity of 90 mm.

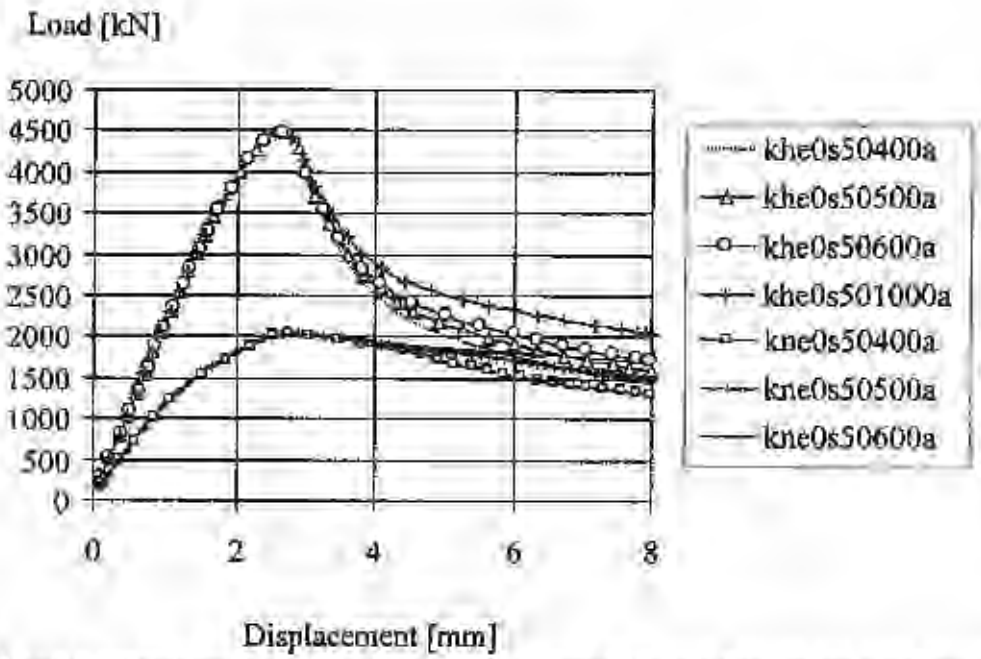

Figure 9 Load displacement relations for cross-sections with reinforcement configuration A and stirrup spacings of 50 mm subjected to pure compression. The yield strength of the stirrups is varied.

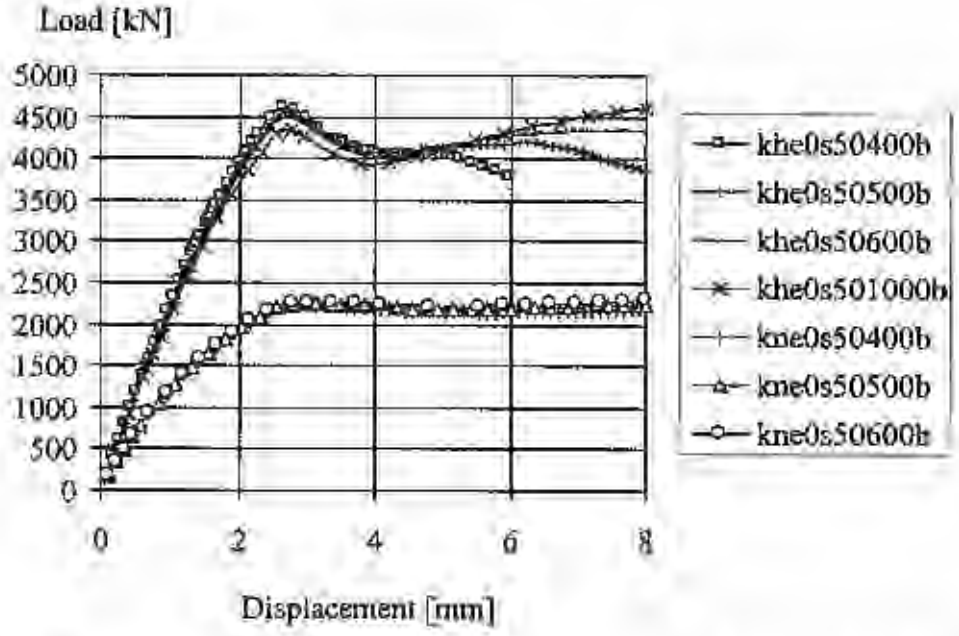

Figure 10 Load displacement relations for cross-sections with reinforcement configuration B and constant stirrup spacings of 50 mm subjected to pure compression. The yield strength of the stirrups is varied.

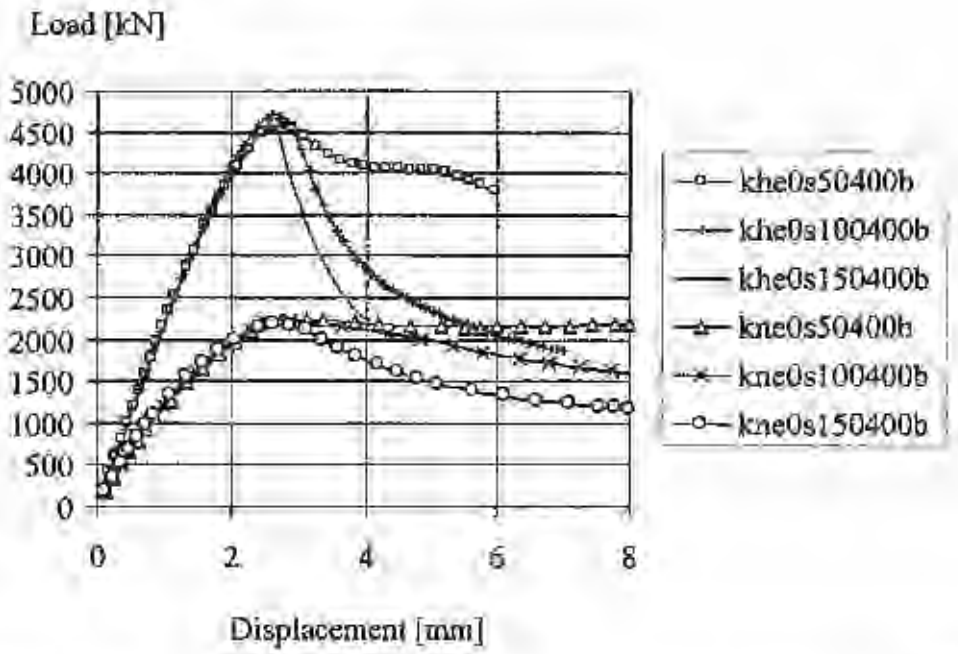

Figure 11 Load displacement relations for cross-sections with reinforcement configuration B and constant stirrup yield strength (400 MPa) subjected to pure compression. The stirrup spacing is varied.

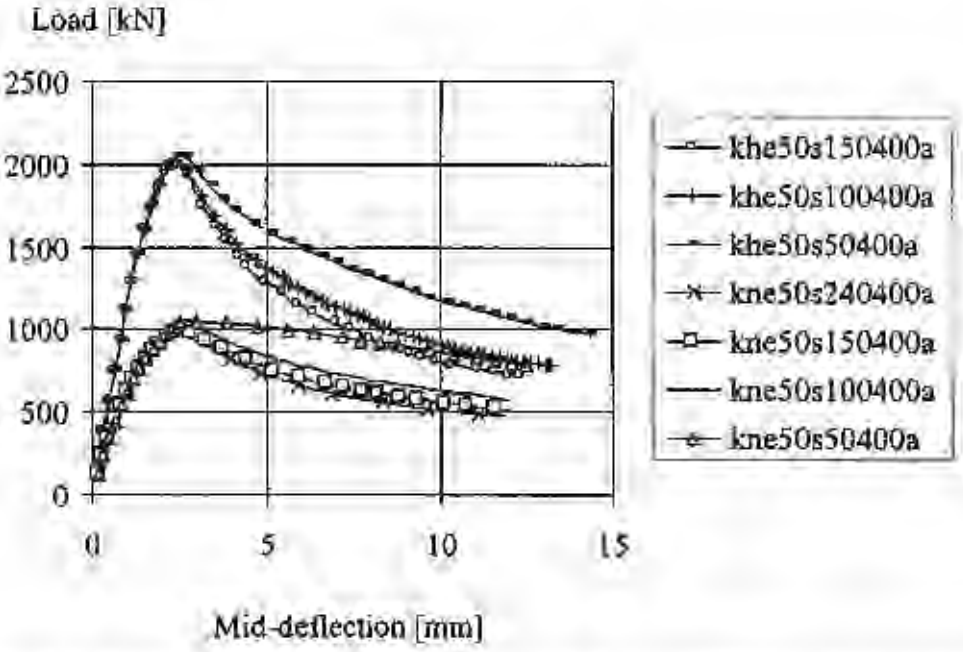

Figure 12 Load deflection relations for cross-sections with reinforcement configuration A and constant stirrup yield strength (400 MPa) subjected to eccentric loading. The stirrup spacing is varied.

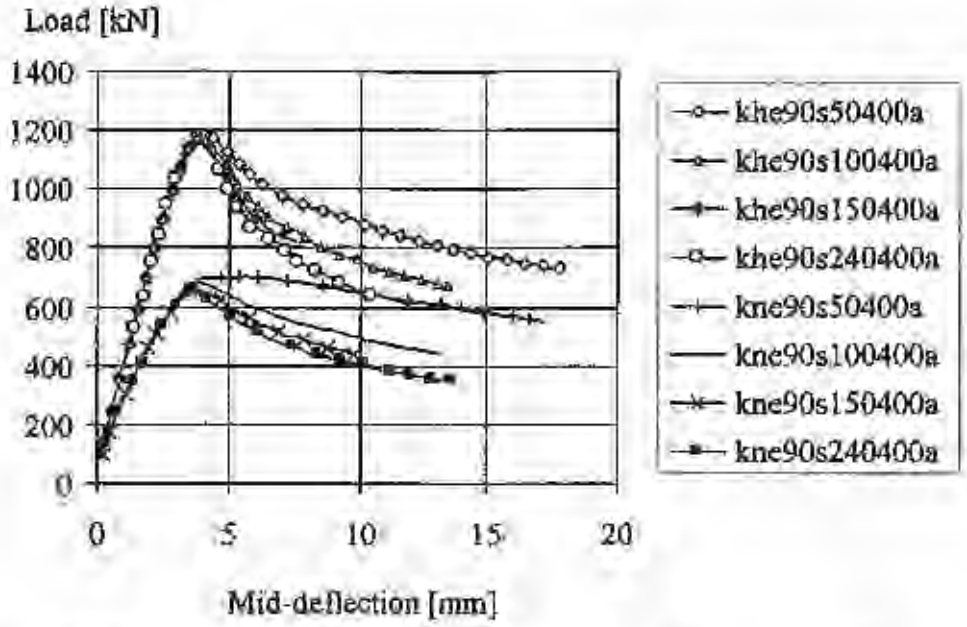

Figure 13 Load deflection relations for cross-sections with reinforcement configuration A and constant stirrup yield strength (400 MPa) subjected to eccentric loading. The stirrup spacing is varied.

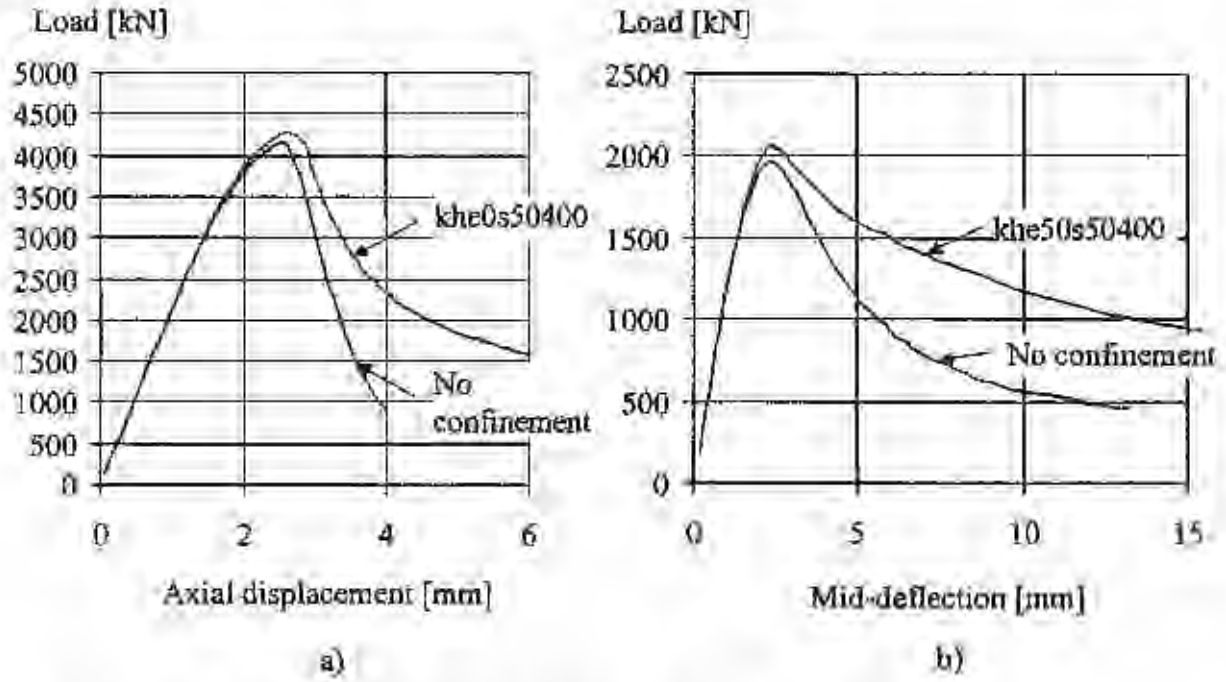

Figure 14 Effect of confinement: a) pure compression, b) eccentricity 50 mm

Figure 14 shows comparisons of cross-sections modeled with and without a confined core. The figure shows the load deflection curves for a high-strength concrete column subjected to pure compression, Figure 14a, and an axial load with eccentricity 50 mm, Figure 14b.

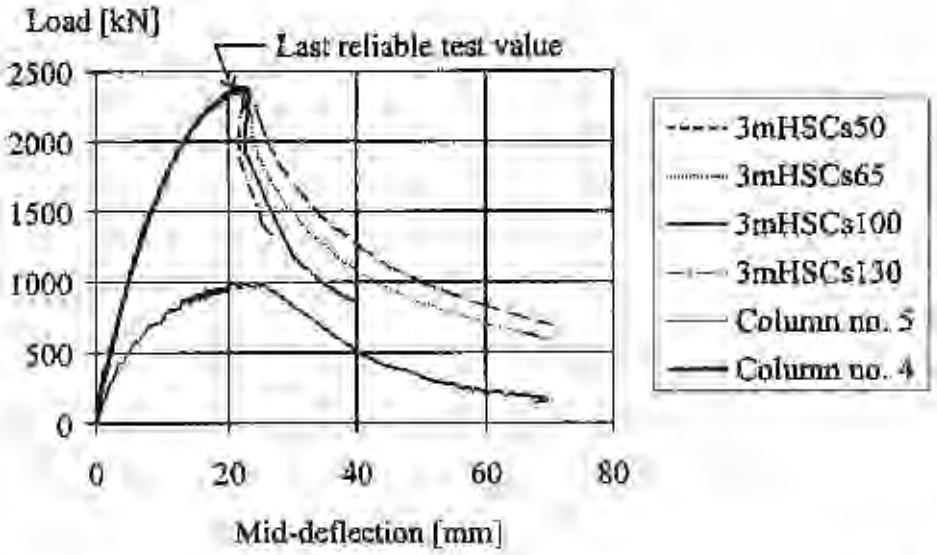

Figure 15 Load deflection relations for a 3 m high-strength concrete column with different stirrup spacings.

So far, only the structural behavior of short columns has been discussed. However, most columns are slender. Figure 15 illustrates the effect of different stirrup spacings for a 3 m long high-strength concrete column subjected to an axial load applied with an eccentricity of 20 mm.

6. DISCUSSION OF RESULTS

Figures 8 through 13 show that closer stirrup spacings have little effect on the maximum load. However, by decreasing the stirrup spacing a less brittle behavior can be achieved. From these figures it can be seen that the greatest effect of confinement is gained in pure compression. Nevertheless, even when the eccentricity is large, the effect of the confinement affects the results. To be able to take advantage of high yield strength steel, it is necessary to design the reinforcement appropriately. This can be seen in Figures 9 and 10.

One of the disadvantages of a high-strength concrete is that it is more brittle than a concrete of a lower strength. For some structures, for example in seismic regions, a ductile behavior in the post-peak region is desirable. To achieve ductility, the volume of stirrups needs to be increased and the reinforcement configuration should be designed to provide high confinement. In the current Swedish code, BBK 94, a maximum stirrup spacing of 15ϕ is allowed, regardless the concrete strength /22/. In tests a ductile behavior of concrete columns of grade K40 has been observed (Claeson /8/). However, as the compressive concrete strength increases, the tendency toward a brittle, sudden failure also increases. Accordingly, the following analysis has been based on the post-peak behavior of a K40 column with the largest spacing allowed. When comparing the results from analyses using high-strength concrete, the post-peak behavior should be at least as ductile as the normal-strength concrete column of grade K40 until the load has decreased to 50% of the maximum load, see Figure 16. Below 50% the risk of a shear or buckling of the reinforcement bars becomes apparent.

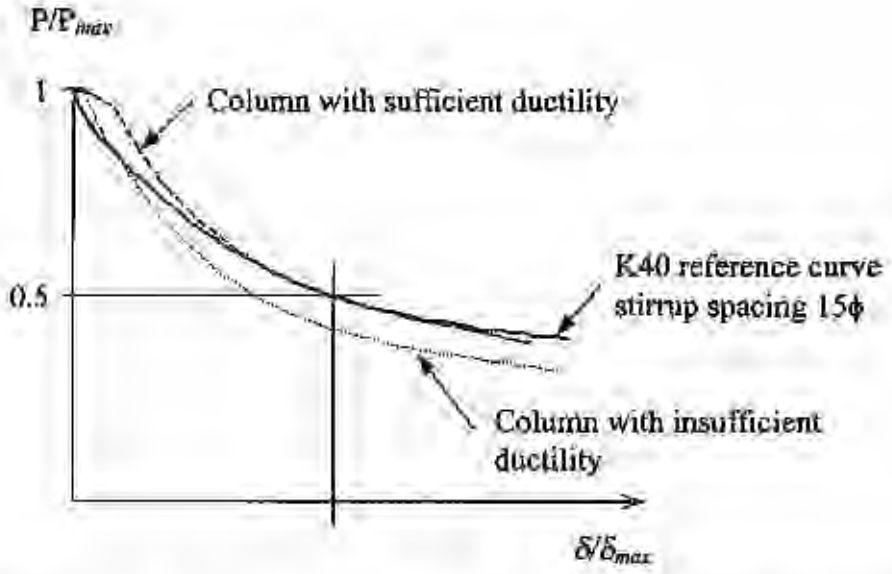

Figure 16 Illustration of a method to determine whether the column of higher strength concrete has sufficient ductility; the reference curve strength is of grade K40 and the stirrup spacing is 15ϕ.

The results of the analyses with different load eccentricities (no second order effects are considered) and concrete strengths are shown in Figure 17. The plot shows the relation between the required volumetric ratio of stirrups in the concrete core and the load eccentricity-to-width ratio for the four concrete strengths. The analyses were based on a stirrup diameter of 8 mm and a stirrup yield strength of 400 MPa. The aim of the plot is to show the minimum volume of stirrups needed for the high-strength concrete (K120) column to obtain the same ductility as the normal-strength concrete column of grade K40. The normal-strength concrete column is designed with stirrups that have the maximum stirrup spacing allowed in the Swedish code BBK 94, 15ϕ. This corresponds to a volumetric stirrup ratio of 0.0052. Since the requirement does not take into account different behaviors due to different concrete strengths, it allows the same spacing even for the highest allowed grade, K80 ($f_{cck} = 56.4$ MPa). It is interesting to note that in the Norwegian code /23/, the maximum stirrup spacing for columns with concrete of grade C65 ($f_{cck} = 54$ MPa) and below is 15ϕ, while this distance is decreased to 10ϕ for concrete strengths above C65. If one assumes that the ductility in the post-peak region of K80 is sufficient, then the difference between this curve and the curve of the high-strength concrete indicates the additional volume of stirrups required. As can be seen from the figure, the volume of stirrups needed decreases with increasing load eccentricity. Therefore, it would be more accurate to propose a required volume of stirrups to secure a ductile post-peak behavior that varies with the load eccentricity and concrete strength. From tests, it has been observed that a normal strength concrete of grade K40 has a desirable post-peak behavior. Accordingly, an effort should be made to obtain this ductility for higher concrete grades. This reasoning indicates that an adjustment is needed for concretes with compressive strengths above K40 that are included in the current code, as well as a new requirement for the high-strength concrete, see Figure 18.

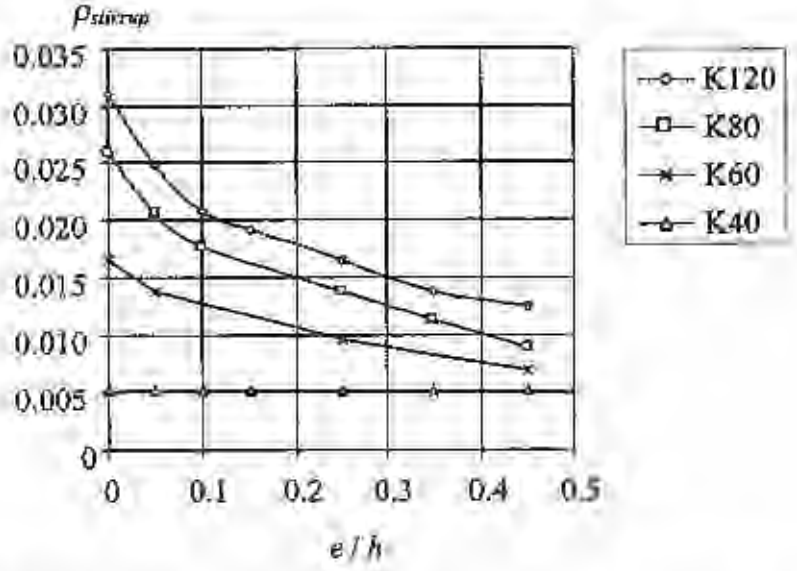

Figure 17 Required volumetric stirrup ratio versus eccentricity-to-width ratio for four different concrete strengths.

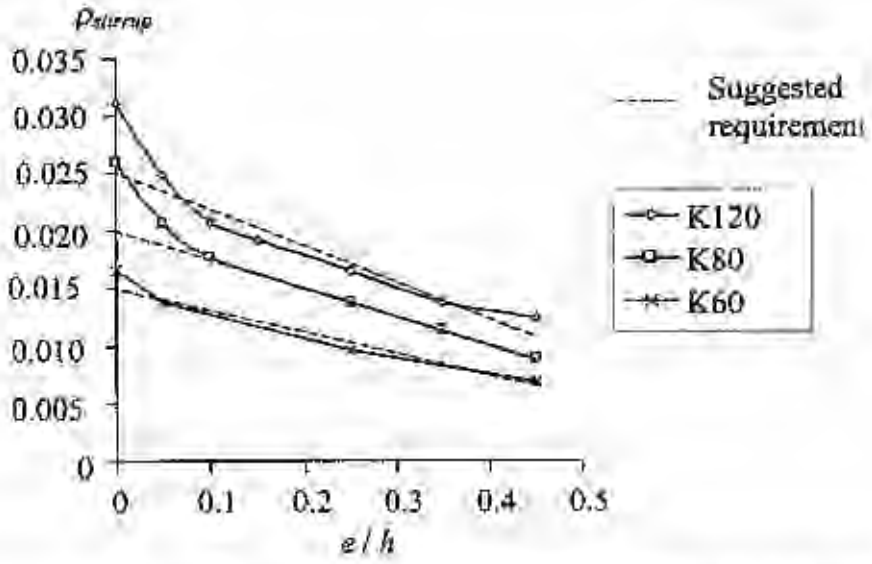

Figure 18 Suggested stirrup volume requirement for different concrete strengths.

However, due to the complexity of the problem, the required volume of stirrups had to be estimated, disregarding the eccentricity of the load, according to the following values:

$$\rho_{stirrup} = 0.025 \text{ for K120} \tag{4}$$

$$\rho_{stirrup} = 0.020 \text{ for K80} \tag{5}$$

$$\rho_{stirrup} = 0.015 \text{ for K60} \tag{6}$$

To validate stirrup requirement curves in Figure 18, a larger cross-section was analyzed, 400 × 400 mm, with the same longitudinal reinforcement ratio (ρ_g) as the smaller cross-section (3.06%). The post-peak curves for the high-strength concrete column and the normal-strength concrete column of grade K40 were compared. From this comparison it could be observed that the proposed volume of stirrups was sufficient to secure a ductile structural behavior in the post-peak region of the high-strength concrete. However, the size effect, both on material and structural level, is still unclear and needs to be further investigated in the future.

7. CONCLUSIONS

The results of the parametric study on reinforced concrete columns presented here allow the following conclusions to be drawn. Generally, a closer stirrup spacing and a denser reinforcement configuration did not contribute to a higher load capacity. However, the cross-section did obtain a greater ductility in the post-peak region. This holds true even for larger load eccentricities for which a well-confined cross-section could benefit from the confining steel. The results presented in this study show that for a well-confined cross-section it is an advantage to use a higher grade of steel, while for a lightly confined section it is not. The most important parameters for obtaining a ductile behavior were the spacing of the stirrups and the reinforcement configuration. It was found that the yield strength of the longitudinal bars had little effect on the post-peak behavior. The results of the FE analysis also show the importance of taking into account that there are two concrete materials in the cross-section, one unconfined for the concrete cover and the other confined for the core. When this was not accounted for, the results gave an overly conservative post-peak behavior.

The volume of stirrups required to achieve the same ductility for a high-strength concrete column as for a column with concrete of grade K40 was studied for different load eccentricities. It was found that the required stirrup volumetric ratio was equal to 0.031 for pure compression and decreased almost linearly to 0.0124 when the load eccentricity-to-width ratio was 0.45 for a concrete of grade K120. It was also observed that a concrete column of grade K80 does not obtain the same ductility as a column of grade K40 unless the volume of stirrups is increased. This is not included in the recommendations given in code BBK 94 today. For practical reasons, the following values are recommended regardless of the value of eccentricity: $\rho_{stirrup}$ = 0.015, 0.020, and 0.025 for K60, K80 and K120, respectively.

ACKNOWLEDGEMENT

The author wishes to thank her advisor, Professor Kent Gylltoft, Head of the Division of Concrete Structures. Thanks are also due to Peter Linde, Ph.D., for his help with the ABAQUS implementation, to Professor P. Paultre at Université de Sherbrooke for his kindness and support during my three month visit, and to Kungliga Vetenskapsakademin (the Royal Academy of Science) for the grant from the Jacob Letterstedt travel grant fund.

NOTATION

The following symbols are used in this paper:

c_x	side dimension of the concrete core parallel to the x-axis
c_y	side dimension of the concrete core parallel to the y-axis
e	eccentricity
f_{cc}	maximum compressive strength of confined concrete in a member
f_{cck}	characteristic compressive cylinder (ϕ150 × 300 mm) strength of unconfined concrete
f_{co}	the compressive cylinder (ϕ150 × 300 mm) strength of unconfined concrete
f_{ct}	maximum tensile concrete strength
f_{hcc}	stress in stirrups at maximum strength of confined concrete
f_l	nominal lateral pressure applied on to the concrete core
f_{le}	effective confinement pressure applied on to the concrete core
f_{sy}	yielding strength of reinforcement bar
G_f	fracture energy of concrete in tension
h	width of cross-section
K_e	confinement effectiveness coefficient
P	axial load
P_{max}	maximum load capacity of the column
s	stirrup spacing
s'	clear vertical spacing between the stirrups
δ	deflection
δ_{max}	deflection at maximum load
ε_c	axial strain in concrete
ε_{cc}	axial strain in confined concrete corresponding to f_{cc}
ε_{co}	axial strain in plain concrete corresponding to f_{co}
ρ_g	volumetric ratio of the longitudinal steel with respect to the volume of the concrete core
$\rho_{stirrup}$	volumetric ratio of stirrups with respect to the volume of the concrete core
σ_c	concrete compressive stress
σ_{ct}	concrete tensile stress
ϕ	diameter
ω_i	clear horizontal spacing between longitudinal bars
ω_{cr}	crack opening displacement

REFERENCES

/1/ Park, R., Priestley, M. J. N., and Gill, W. D., "Ductility of Square-confined Concrete Columns," *ASCE Journal of the Structural Division*, 108(4), 1982, pp. 929-950.

/2/ Sheikh, S.A., and Uzumeri, S.M., "Analytic Model for Concrete Confinement in Tied Columns," *ASCE Journal of the Structural Division*, 108(12), 1982, pp. 2703-2722.

/3/ Yong, Y.K., Nour, M.G., and Nawy, E.G., "Behavior of Laterally Confined High-Strength Concrete Under Axial Loads," *ASCE Journal of the Structural Division*, 114(2), 1988, pp. 332-351.

/4/ Bjerkeli, L., Tomaszewicz, A., and Jensen, J.J., "Deformation Properties and Ductility of High Strength Concrete," *Proceedings, Second International Symposium on Applications of High Strength Concretes*, Berkeley, 1990, pp. 215-238.

/5/ Madas, P., and Elnashai, A. S., "A New Confinement Model for the Analysis of Concrete Structures Subjected to Cyclic and Transient Dynamic Loading," *Earthquake Engineering and Structural Dynamics*, Vol. 21, 1992, 409-431.

/6/ Cusson, D., and Paultre, P., "High-Strength Concrete Columns Confined by Rectangular Ties," *ASCE Journal of Structural Engineering*, Vol. 120, No. 3, March, 1994, pp. 783-804.

/7/ HKS, Hibbit, Karlsson and Sorensen INC., "ABAQUS, Theory Manual, Version 5.6," HKS, Providence, Rhode Island, USA, 1996.

/8/ Claeson, C., "Behavior of Reinforced High Strength Concrete Columns." Publication 95:1. Division of Concrete Structures, Chalmers University of Technology, 1995, 54 pp.

/9/ Mustapha, R., "Spalling of the Cover of High-Strength Concrete Columns: Effects of Curing Conditions," Master's Thesis 96:8. Division of Concrete Structures, Chalmers University of Technology, Sweden, 1996, 70 pp.

/10/ Oresten, J., "Provning och Analys av Slanka Pelare i Högpresterande Betong," Examensarbete 93:4. (Tests and Analysis of Slender Columns of High Performance Concrete. Master's thesis 93:4). Division of Concrete Structures, Chalmers University of Technology, Sweden, 1993, 73 pp. (In Swedish)

/11/ Popovics, S., "A Numerical Approach to the Complete Stress-Strain Curve of Concrete," *Cement and Concrete Research*, 3(5), 1973, pp. 583-599.

/12/ Fafitis, A., and Shah, S.P., "Lateral Reinforcement for High-Strength Concrete Columns," *ACI Special Publication* SP 87-12, 1985, pp. 213-232.

/13/ Richart, F. E., Brandtzaeg, A., and Brown, R. L., "A Study of the Failure of Concrete under Combined Compressive Stresses," *Bulletin* No. 185, Engineering Experimental Station, University of Illinois, Urbana, 1928, 104 pp.

/14/ ACI Committee 318 "Building Code Requirements for Reinforced Concrete," ACI 318-95, and Commentary, ACI 318R-95, American Concrete Institute, Detroit, 1995, 353 pp.

/15/ Légéron, F., and Paultre, P., "Analytical Model for Confined Concrete Columns," *Proceedings of the 1997 Conference of the Canadian Society for Civil Engineering*, Sherbrooke, Québec, Canada, May 28-30, Vol. 4, 1997, pp. 379-388.

/16/ Hillerborg, A., Modéer, M., and Petersson, P-E., "Analysis of Crack Formation and Crack Growth in Concrete by Means of Fracture Mechanics and Finite Elements," *Cement and Concrete Research*, Vol. 6, 1976, pp. 773-782.

/17/ Gylltoft, K., "Fracture Mechanics Models for Fatigue in Concrete Structures," Division of Structural Engineering, Luleå University of Technology, Doctoral Thesis 1983:25D, 1983, 210 pp.

/18/ Richart, F. E., and Brown, R. L., "An Investigation of Reinforced Concrete Columns," University of Illinois Engineering Experimental Station, *Bulletin* No. 267, June, 1934, 91 pp.

/19/ Hognestad, E., "A Study of Combined Bending and Axial Load in Reinforced Concrete Members," University of Illinois Engineering Experimental Station, *Bulletin* No. 399, June, 1951, 128 pp.

/20/ Karr, P. H., Hanson, N. W., and Capell, H. T., "Stress-Strain Characteristics of High Strength Concrete," *Douglas McHenry International Symposium on Concrete and Concrete Structures*, ACI SP-55, American Concrete Institute, Detroit, 1978, pp. 161-185.

/21/ Mak, S. L., Attard, M. M., Ho, D. W. S., and Darwall, P. leP., "Effective In-situ Strength of High Strength Concrete Columns," *Australian Civil Engineering Transactions*, Vol. CE35 No.2, 1993, pp. 87-94.

/22/ BBK 94 "Boverkets Handbok för Betongkonstruktioner," 1994, Band 1 and 2 (Manual for Concrete Structures from the Swedish Board of Housing, Building and Planning, 1994, Volumes 1 and 2). (In Swedish)

/23/ NS 3473 "Prosjektering av Betongkonstruksioner Beregnings- og konstruksjonsregler," Norsk standard, NBR, Norway, 1992, 103 pp. (In Norwegian)